DMD Fast Forward. Published on January 3, 2020 as DOI: 10.1124/dmd.119.089193
This article has not been copyedited and formatted. The final version may differ from this version.

Title page

MRP3 Is Responsible for the Efflux Transport of Curcumin Glucuronide from Hepatocytes to the Blood

YU-MENG JIA, TING ZHU, HUAN ZHOU, JIN-ZI JI, TING TAI, HONG-GUANG XIE ID

Division of Clinical Pharmacology, General Clinical Research Center, Nanjing First Hospital, Nanjing Medical University (Y.-M.J., J.-Z.J., T.T., H.-G.X.); Department of Clinical Pharmacy, School of Basic Medicine and Clinical Pharmacy, China Pharmaceutical University (Y.-M.J., T.Z., H.Z., H.-G.X.); and Department of Clinical Pharmacy, Nanjing Medical University School of Pharmacy (H.-G.X.), Nanjing, People's Republic of China

DMD Fast Forward. Published on January 3, 2020 as DOI: 10.1124/dmd.119.089193
This article has not been copyedited and formatted. The final version may differ from this version.

Running title: MRP3 transports curcumin glucuronide

Corresponding author: Dr. Hong-Guang Xie, General Clinical Research Center, Nanjing First Hospital, Nanjing Medical University, 68 Changle Road, Nanjing 210006, People's Republic of China. Tel: +86-25-52887034; fax: +86-25-52269924. E-mail: hongg.xie@gmail.com, or hong-guang.xie@njmu.edu.cn

Hong-Guang Xie (https://orcid.org/0000-0002-1089-9457)

Number of text pages: 34

Words in the Abstract: 213

Words in the Introduction: 484

Words in the Discussion: 998

Number of references: 29

Number of Tables: 1

Number of Figures: 5

Number of Supplementary Tables: 2

ABBREVIATIONS:

ABCC3, ATP-binding cassette, subfamily C, member 3; AMP, adenosine monophosphate; ATP, adenosine triphosphate; $AUC_{0\text{-}t}$, area under the plasma drug concentration-time curve to last time point measured; $AUC_{0\text{-}\infty}$, area under the plasma drug concentration-time curve extrapolated to infinity; BCRP, breast cancer resistance protein; C_{max}, the maximum plasma drug concentration (observed); COG, curcumin-*O*-glucuronide; CUR, curcumin; $E_2$17βG, estradiol-17β-D-glucuronide; F, systemic bioavailability; HPLC, high-performance liquid chromatography; IS, internal standard; KO, knock-out, or knockout; LC-MS/MS, liquid chromatography with tandem mass spectrometry; MRP, multidrug resistance-associated protein; MS, mass spectrometry; *m*/*z*, the ratio of mass to (electronic) charge; PCR, polymerase chain reaction; P-gp, P-glycoprotein; qRT-PCR, quantitative reverse transcription-polymerase chain reaction; $t_{½}$, half-life; T_{max}, time needed to reach the maximum plasma drug concentration (observed); UGT, uridine diphosphate-glucuronosyltransferase; WT, wild-type.

ABSTRACT

Curcumin, a major polyphenol present in turmeric, is predominantly converted to curcumin-*O*-glucuronide (COG) in enterocytes and hepatocytes via glucuronidation. COG is a principal metabolite of curcumin in plasma and faeces. It appears that the efflux transport of the glucuronide conjugates of many compounds is mediated largely by MRP3 (multidrug resistance-associated protein 3, the gene product of the *Abcc3*). However, it is currently unknown whether this was the case with COG. In this study, Mrp3 knock-out (KO) and wild-type (WT) mice were used to evaluate the pharmacokinetics profiles of COG, the liver-to-plasma ratio of COG, and the COG-to-curcumin ratio in plasma, respectively. The ATP-dependent uptake of COG into recombinant human MRP3 inside-out membrane vesicles was measured for further identification, with estradiol-17β-D-glucuronide used in parallel as the positive control. Results showed that plasma COG concentrations were extremely low in KO mice compared to WT mice, that the liver-to-plasma ratios of COG were 8-fold greater in KO mice than in WT mice, and that the ATP-dependent uptake of COG at 1 or 10 μM was 5.0- and 3.1-fold greater in the presence of ATP than in the presence of AMP, respectively. We conclude that Mrp3 is identified to be the main efflux transporter responsible for the transport of COG from hepatocytes into the blood.

SIGNIFICANCE STATEMENT

This study was designed to determine whether Mrp3 could be responsible for the efflux transport of curcumin-*O*-glucuronide, a major metabolite of curcumin present in plasma and faeces, from hepatocytes into the blood using Mrp3 knock-out mice. In this study, curcumin-*O*-glucuronide was identified as a typical Mrp3 substrate. Results suggest that herb-drug interactions would occur in patients concomitantly taking curcumin and either an MRP3 substrate/inhibitor or a drug that is glucuronidated by UGTs predominantly.

DMD Fast Forward. Published on January 3, 2020 as DOI: 10.1124/dmd.119.089193
This article has not been copyedited and formatted. The final version may differ from this version.

Introduction

Curcumin (CUR), the main bioactive ingredient of the spice turmeric (*Curcuma longa* L.), possesses a broad spectrum of biological and pharmacological activities, including, but not limited to antioxidant, anticancer, anti-inflammatory, antidiabetic, hepatoprotective, and lipid-lowering effects and more (Farzaei, et al., 2018; Kunati, et al., 2018; Ozawa, et al., 2017; Huang, et al., 2018). However, CUR exhibits extremely poor systemic bioavailability ($F < 1\%$) in rodents and humans due to its alkaline instability, poor aqueous solubility, low oral absorption, and rapid metabolism (Anand, et al., 2007). Despite its limited use in clinical settings (Garcea, et al., 2005; Irving, et al., 2013), CUR is still extensively used as an herbal medicine (e.g. a cancer chemopreventive agent) and as a dietary supplement for food coloring in Southeastern Asian areas (Mahale, et al., 2018b).

Evidence has demonstrated that oral CUR is principally converted to curcumin-*O*-glucuronide (COG) (see Fig. 1) by certain UGTs (UDP-glucuronosyltransferases) (Hoehle, et al., 2007; Lu, et al., 2017). In addition, CUR is reduced by certain reductases to dihydrocurcumin, tetrahydrocurcumin, and hexahydrocurcumin (Mahale, et al., 2018a). Of them, COG is a primary circulating metabolite in rodents and humans (Ireson, et al., 2002; Mahale, et al., 2018b). Studies have further demonstrated that CUR metabolites (predominantly COG) activate CYP3A4 activity (Hsieh, et al., 2014), and that oral intake of CUR would significantly decrease the systemic bioavailability of CYP3A4 substrate drugs, such as everolimus (an immunosuppressant) (Hsieh, et al., 2014). On the other hand, as an inhibitor of UGT1A and of non-selective kinase (Abe, et al., 2011), CUR suppresses the glucuronidation of many (if not all) compounds in the body. For example, concomitant use of CUR decreases glucuronidation of acetaminophen (Volak, et al., 2010) and mycophenolic acid (Basu, et al., 2007). Clearly, thorough elucidation of the transport

and elimination of COG would help us better understand herb-drug interactions involved and their underlying mechanisms.

COG is cleared predominantly via biliary and faecal excretion, with evidence of the presence of the enterohepatic recycling (Bangphumi, et al., 2016; Sharma, et al., 2007), a process in which the canalicular membrane efflux transporters MRP2 and BCRP of hepatocytes are involved (Roberts, et al., 2002). Despite recent public interest and widespread consumption of CUR around the world, little is known about how COG molecules formed intracellularly move out for clearance. MRP3, expressed dominantly on the basolateral membrane side of enterocytes and the sinusoidal membrane of hepatocytes, functions as an efflux transporter that mediates the efflux transport of certain compounds from hepatocytes into the blood for further renal excretion. Since MRP3 prefers transporting the glucuronide conjugates of endogenous or exogenous compounds (Zelcer, et al., 2006), it was postulated that COG might be a substrate of MRP3. To test such a hypothesis, we used Mrp3 knock-out (KO) and wild-type (WT) mice to evaluate differences in their pharmacokinetic parameters of COG, the liver-to-plasma ratios of CUR and those of COG, respectively, after oral administration of CUR. To further confirm the findings from mice, we measured the adenosine triphosphate (ATP)-dependent uptake of COG by using recombinant human MRP3 inside-out membrane vesicles in vitro.

DMD Fast Forward. Published on January 3, 2020 as DOI: 10.1124/dmd.119.089193
This article has not been copyedited and formatted. The final version may differ from this version.

Materials and Methods

Chemicals and reagents. CUR and estradiol-17*β*-D-glucuronide ($E_2$17βG) were purchased from Sigma-Aldrich (St. Louis, MO, USA). COG was the product of Toronto Research Chemicals (Toronto, Ontario, Canada). Hesperetin (used as the internal standard, or IS) was provided by Aladdin (Shanghai, China). Recombinant human MRP3 inside-out membrane vesicles GM0021-V (GenoMembrane, Yokohama, Japan), adenosine monophosphate (AMP), and ATP were supplied by Solvo Biotechnology (Szeged, Hungary). Analytical-grade formic acid, high-performance liquid chromatography (HPLC)-grade acetonitrile, and methanol were from Merck (Darmstadt, Germany). Deionized water was purified using the Millipore Milli-Q system (Millipore, Milford, MA, USA).

Study animals. All animal care and study protocol were approved by the Experimental Animal Welfare and Ethics Committee, Nanjing Medical University, and conducted in compliance with the Guidelines for Animal Experimentation, Nanjing Medical University, China. The Mrp3 KO mice were generously supplied by the Netherlands Cancer Institute, Amsterdam, the Netherlands. The WT mice of FVB strain were purchased from Vital River Laboratories, Beijing, China. All animals were housed in an officially accredited experimental animal facility under air-controlled conditions with a 12-h light/dark cycle, ambient temperature maintained at 22 – 24℃, and relative humidity of 40 – 60%. All study mice had free access to standard rodent food and tap water, but they were fasted for 12 h before the initiation of all studies.

Pharmacokinetics study of COG in mice. For mouse studies, the frequently used dosage of CUR ranges from 20 to 400 mg/kg (Szymusiak, et al., 2016; Mahale, et al., 2018a). Accordingly, a dose

of 200 mg/kg was chosen as a moderate dose for mice in this study. Male Mrp3 KO and WT mice (aged 6 – 8 weeks) were administered with 200 mg/kg of CUR by oral gavage (n = 8 each) based on a similar study (Szymusiak, et al., 2016). After oral dosing, a series of blood samples (30 μL each) were withdrawn from the orbital venous plexus at 0.083, 0.25, 0.5, 1, 2, 4, 8, 12, and 24 h, respectively, and collected into heparinized tubes. Plasma samples were obtained after centrifugation at 4000 rpm for 10 min and stored at –80 ^{o}C until analysis.

Quantification of CUR and COG in plasma and liver samples of mice. Again, male Mrp3 KO and WT mice (aged 6 – 8 weeks; n = 8 each) were administered with a single dose of CUR at 200 mg/kg by oral gavage. Thereafter, blood samples (100 μL each) were withdrawn from the orbital venous plexus at 1 h after dosing, and liver specimens (approximately 200 mg each) were collected shortly after sacrifice as described elsewhere (Ji, et al., 2018). Liver tissues were weighed and homogenized with ice-cold normal saline solution containing 0.1% formic acid (20%, w/v) to keep COG stable. All plasma and liver samples were separated after centrifugation at 4000 rpm for 10 min and the supernatants were stored at –80 ^{o}C until analysis.

Measurements of the mouse mRNA expression levels of the efflux transporters of interest. Liver and intestinal specimens (approximately 200 mg each) were collected shortly after sacrifice as described elsewhere (Ji, et al., 2018), and were stored at –80 ^{o}C until analysis. To determine whether *Abcc3* gene deletion could significantly modulate the expression levels of the genes that encode the efflux transporters of interest, including the *Abcc1*, *Abcc2*, and *Abcg2*, we measured the mRNA expression levels in the intestine and liver of the *Abcc3* KO versus WT mice using quantitative reverse transcription polymerase chain reaction (qRT-PCR). In brief, the extraction of

DMD Fast Forward. Published on January 3, 2020 as DOI: 10.1124/dmd.119.089193
This article has not been copyedited and formatted. The final version may differ from this version.

total RNA and subsequent synthesis of complementary DNA (cDNA) were described elsewhere (Tai, *et al*., 2016) according to the protocols from the manufacturers. The primer sequences for the genes tested and the internal reference gene *Gapdh* were shown in Supplementary Table 1. PCR amplification and melting analysis were conducted using ABI 7500 real-time PCR apparatus (Applied Biosystems, Carlsbad, CA, USA) as detailed elsewhere (Tai, *et al*., 2016). The mRNA expression level was represented by a Ct value (defined as the number of PCR cycles that have crossed an arbitrarily chosen signal threshold in the log phase of the amplification curve), and relative expression of a target gene was expressed as a fold change, which was calculated using the following equation: fold change = $2^{-\Delta\Delta Ct}$, where $\Delta Ct = Ct_{(target)} - Ct_{(gapdh)}$.

The active uptake of COG into the inverted (inside-out) human MRP3 membrane vesicles. The vesicular uptake studies were performed using the rapid filtration technique as described previously (Ji, et al., 2018). The "reaction buffer" (Solvo kit) consisted of 50 mM MOPS−Tris, 70 mM KCl, and 7.5 mM $MgCl_2$, 10 mM ATP (or AMP), COG (1 or 10 μM), $E_2$17βG (4 μM, as the positive control), and recombinant human MRP3 membrane vesicles (inside-out). Human MRP3 vesicle suspensions were loaded onto the 96-well flat bottom of the tissue culture plates. After preincubation at 37 ^oC for 5 min, the reactions were initiated by the addition of the compound tested in the presence of ATP or AMP at 37 ^oC for 5 min and stopped by the addition of 200 μL of ice-cold "washing mix" (Solvo kit) containing 400 mM MOPS−Tris and 700 mM KCl. Samples were then transferred to the 96-well glass-fiber filter plate and filtered using a Multiscreen HTS vacuum manifold (Millipore, Billerica, MA, USA). The filters were washed with an ice-cold "washing mix" 5 times. The MRP3 vesicles on the filters were extracted by 80% acetonitrile at room temperature, and the supernatants were collected after centrifugation at 2000 rpm for 2 min. The ATP-dependent uptake of the testing compound into recombinant human MRP3 membrane

DMD Fast Forward. Published on January 3, 2020 as DOI: 10.1124/dmd.119.089193
This article has not been copyedited and formatted. The final version may differ from this version.

vesicles was measured by LC-MS/MS method (see below for details). The uptake assays were performed in triplicate, and all data are presented as mean ± SD.

The amount of CUR or COG transported by the inverted membrane vesicles of MRP3 was calculated using the following formula:

the uptake activity (pmol/min/mg protein) = A – B; and

the uptake ratio = A/ B

where "A" refers to the transported amount of a testing compound in the presence of ATP, and "B" refers to the transported amount of the same testing compound in the presence of AMP, both of which were normalized to the incubation time (min) and the amount of total vesicular protein (mg).

In this study, the measured uptake ratio of $E_2 17\beta G$ was greater than 2-fold as required as the positive control, indicating that the incubation system used worked well and that data generated was reliable and reproducible. Similarly, for the compound to be tested, if its uptake ratio in the presence of ATP was greater than 2-fold than that in the presence of AMP, that compound would be considered a substrate of human MRP3.

Sample preparation. For the preparation of plasma and liver samples, an aliquot of 10 μL sample was spiked with 100 μL acetonitrile (containing 0.1% formic acid and 30 ng/mL hesperetin as the IS). For the preparation of MRP3 vesicles, an aliquot of 30 μL sample was spiked with 60 μL acetonitrile (containing 30 ng/mL hesperetin as the IS). All samples were vortex-mixed for 3 min and subsequently centrifuged at 4000 rpm at 4 ^{o}C for 10 min. The resulting supernatants were centrifuged at 14000 rpm for 20 min at 4 ^{o}C. Finally, an aliquot of 5 μL was injected into LC-MS/MS system for quantification.

DMD Fast Forward. Published on January 3, 2020 as DOI: 10.1124/dmd.119.089193
This article has not been copyedited and formatted. The final version may differ from this version.

LC-MS/MS conditions for the quantification of CUR, COG, and $E_2$17βG. The amount of CUR, COG, and $E_2$17βG was quantified by a LC-MS/MS system, which was equipped with a Shimadzu LC–30A Series system (Shimadzu, Kyoto, Japan) and a Sciex API 4500 tandem mass spectrometer (Applied Biosystems, Foster City, CA, USA). Chromatographic separation was achieved at 40 °C on a Poroshell 120 SB-C18 column (100 × 2.1 mm, 2.7μm). The eluant was 0.1% formic acid in water (solvent A) and 0.1% formic acid in acetonitrile (solvent B). The gradient elution was set as follows: solvent B being increased from 20% to 90% at 0.01 – 2.30 min, maintained 90% at 2.31 – 4.50 min, then declined to 20% at 4.51 min, and maintained at 20% until the end of elution at 5.50 min, at a flow rate of 0.3 mL/min. The temperature of the auto-sampler was maintained at 4°C, and the injection volume was 5 μL. The MS was operated using an electron spray ionization source with multiple reaction monitoring mode in negative ion mode. The MS parameters were ion-spray voltage at – 4500 V, ion source temperature 400°C, and curtain gas, collision gas, ion source gas-1 and -2 set at 15, 8, 50, and 55 Psi, respectively. The compound-selective MS parameters were optimized and are summarized in Supplementary Table 2.

Statistical analysis. Data are presented as mean ± SD. Pharmacokinetic parameters of COG were analyzed for each mouse by Phoenix WinNonlin version 6.1 (Pharsight Co., Ltd., Mountain View, CA, USA) using a non-compartmental analysis (NCA) model. Statistical analyses were performed using unpaired Student's *t* test for the group comparison of a single variable. A two-tailed *P* value of less than 0.05 is considered statistically significant.

DMD Fast Forward. Published on January 3, 2020 as DOI: 10.1124/dmd.119.089193
This article has not been copyedited and formatted. The final version may differ from this version.

Results

Impaired efflux transport of COG in Mrp3 KO mice. Since MRP3 preferentially transports its substrates (e.g., glucuronide conjugates) from enterocytes and hepatocytes into the blood, it was predicted that plasma COG concentrations would be significantly lower in Mrp3 KO mice than in WT mice after oral dosing of CUR. Illustrated in Fig. 2 are the mean plasma COG concentration-time curves in Mrp3 KO versus WT mice after receiving an oral dose of 200 mg/kg CUR, with the pharmacokinetics parameters summarized in Table 1. As expected, the maximum plasma COG concentrations (C_{max}) were 32-fold lower in KO mice than in WT mice ($P < 0.001$), $AUC_{0\text{-}t}$ values of COG were approximately 25-fold lower in KO mice than in WT mice, but elimination half-life ($t_{1/2}$) was significantly prolonged in KO mice relative to WT mice. However, CUR pharmacokinetics was not analyzed because of low levels and high variation of unconjugated CUR in mouse plasma samples. These data suggest that systemic exposure of COG in plasma is significantly decreased in Mrp3 KO mice in comparison to WT mice, demonstrating that the efflux transport of COG formed in hepatocytes is almost abrogated due to knockout of the *Abcc3* gene in mice.

Mrp3-mediated efflux transport of COG identified in vivo and in vitro. Considering that the hepatocyte Mrp3 transports its substrates from hepatocytes into the blood, the liver-to-plasma ratio of mice is generally recognized as the gold standard for determining whether a compound could be the substrate of Mrp3 as described elsewhere (Ji, et al., 2018). As shown in Fig. 3A, the liver-to-plasma ratios of COG and those of CUR were determined in the presence or absence of Mrp3 in mice. Results indicated that the liver-to-plasma ratios of COG were 8-fold greater in Mrp3 KO mice than in WT mice, suggesting that COG is a substrate of Mrp3. As shown in Fig. 3A, there were no marked differences in the liver-to-plasma ratios of CUR between Mrp3 KO and WT mice,

DMD Fast Forward. Published on January 3, 2020 as DOI: 10.1124/dmd.119.089193
This article has not been copyedited and formatted. The final version may differ from this version.

indicating that CUR is not a substrate of Mrp3. On the other hand, the COG-to-CUR ratios in plasma of KO mice were significantly low compared to those of WT mice (Fig. 3B), opposite to their changes in the liver, further suggesting that COG is a substrate of Mrp3.

To confirm that COG is also an MRP3 substrate in humans, inverted membrane vesicles that overexpress human MRP3 were used to evaluate the ATP-dependent uptake of COG. As a well-characterized MRP3 substrate, $E_2$17βG was used in parallel as the positive control to further validate the incubation system used and data derived in this study. As shown in Fig. 4A, the ATP-dependent uptake of $E_2$17βG was 4.6-fold greater in the presence of ATP than in the presence of AMP, indicating that the vesicular transport assay used was reliable. After incubation with 1 or 10 μM COG in the MRP3-overexpressing vesicles, the uptake activity of MRP3 was 5.0- and 3.1-fold higher in the presence of ATP than in the presence of AMP, respectively. As shown in Fig. 4B, the uptake ratio of COG was greater than 2-fold when added at a concentration of 1 or 10 μM as did $E_2$17βG. These data confirmed that COG is a substrate of human MRP3 in vitro.

Similar levels of the *Abcc2* and *Abcg2* mRNA expression between Mrp3 KO and WT mice. To further investigate the possible effects of the *Abcc3* gene deletion on other relevant transporters in mice, the mRNA expression levels of the four genes of interest (*Abcc1*, *Abcc2*, *Abcc3*, and *Abcg2*) were measured with normalization against the mRNA expression level of the reference gene *Gapdh* and subsequently were compared between the *Abcc3* KO and WT mice. As shown in Fig. 5, except for the lack of *Abcc3* mRNA expression in the *Abcc3* KO mice as anticipated, there were no marked differences in the mRNA expression levels of the other genes tested between the *Abcc3* KO and WT mice, suggesting that *Abcc3* gene disruption seems not to modulate the expression of the genes evaluated.

DMD Fast Forward. Published on January 3, 2020 as DOI: 10.1124/dmd.119.089193
This article has not been copyedited and formatted. The final version may differ from this version.

Discussion

The most significant finding of this study is that MRP3 is responsible exclusively for the efflux transport of COG using an Mrp3 KO mouse model and recombinant human MRP3 inverted membrane vesicles, revealing a critical role of MRP3 in the efflux transport of COG in the body. These novel findings would be used to better explain herb-drug interactions in patients when concomitantly taking CUR and any other drugs known to be MRP3 inhibitors and/or substrates, or drugs whose main metabolic pathway is glucuronidation. In terms of the widespread use of CUR in the Southeastern Asians, such herb-drug interactions seem to be very important.

COG, generated in enterocytes and hepatocytes by UGTs (Lu, et al., 2017), is transported to the blood, in turn, by the basolateral membrane transporter MRP3 of enterocytes and the sinusoidal plasma membrane transporter MRP3 of hepatocytes, consequently leading to a dramatic increase in its systemic exposure. As summarized in Table 1, compared to WT mice, Mrp3 KO mice exhibited significantly declined systemic exposure of COG (reflective of decreased AUC and C_{max}) and extended elimination process (increased $t_{1/2}$), consistent with expected results. As shown in Fig. 2, plasma COG concentrations were extremely low (close to the lower limit of quantification) in Mrp3 KO mice, indicating that the efflux transport of COG formed inside cells is mediated exclusively by Mrp3. In theory, for Mrp3 KO mice, the liver-to-plasma ratio of COG would be elevated significantly, and the plasma COG-to-CUR ratio would be decreased. In this study, there was complete consistency between the observed and expected results.

Evidence has demonstrated that Mrp2 is involved in the biliary excretion of COG (Lee, et al., 2012). To determine whether blunted sinusoidal transport of COG to the blood in hepatocytes of Mrp3 KO mice could be compensated with markedly increased biliary elimination as a result of

enhanced expression of other efflux transporters (such as Mrp2 and Bcrp) that are expressed on the basolateral membrane of hepatocytes. It is not the case. In this study, the mRNA expression levels of several relevant efflux transporters were measured with the liver and intestinal samples for comparison between the two groups (Mrp3 KO vs. WT mice). As shown in Fig. 5, there were no significant differences in the mRNA expression levels of the genes *Abcc2* (encoding Mrp2) and *Abcg2* (encoding Bcrp) between the two groups, consistent with earlier observations that hepatic Mrp2 expression levels are not different between Mrp3 KO and WT mice (Zelcer, et al., 2006), and that the biliary excretion of diclofenac acyl glucuronide (a known Mrp2 substrate) was similar between the Mrp3 KO and WT mice (Seitz, et al., 1998). Similar to the case of diclofenac acyl glucuronide, Mrp2-mediated efflux transport of COG (also a Mrp2 substrate) (Lee, et al., 2012) from hepatocytes to the bile was not enhanced in Mrp3 KO mice relative to WT mice. The above evidence strongly suggests that *Abcc3* gene deletion seems not to affect the expression level and transport activity of Mrp2.

Although CUR is an inhibitor and substrate of BCRP (Karibe, et al., 2018; Berginc, et al., 2012), no evidence is currently available showing that COG is a substrate of BCRP. In our preliminary study, there were no marked differences in the *Abcg2* mRNA expression levels of hepatocytes and enterocytes between the Mrp3 KO and WT mice (see Fig. 5), implying the lack of the anticipated increases in the Bcrp-mediated biliary excretion of COG in Mrp3 KO mice.

In the gut mucosa and epithelial cells, ingested CUR is converted to COG by the intestinal UGTs (i.e., UGT1A7, UGT1A8, and UGT1A10) (Lu, et al., 2017), which is transported, in turn, to the blood via Mrp3 expressed on the basolateral membrane of enterocytes, or back to the gut lumen via the efflux transporters (such as Mrp2 and Bcrp) expressed on the apical side of enterocytes, where the enterohepatic circulation of COG would occur (Bangphumi, et al., 2016).

DMD Fast Forward. Published on January 3, 2020 as DOI: 10.1124/dmd.119.089193
This article has not been copyedited and formatted. The final version may differ from this version.

Furthermore, COG formed in hepatocytes is transported to the blood via Mrp3 expressed on the sinusoidal side of hepatocytes, and to the bile via Mrp2 and Bcrp on the apical side of hepatocytes. Drug metabolism and transport are simultaneous in the body, and their entire processes are dynamic over time. The interplay between one transporter and another, and between drug metabolism and drug transport in the body would be more complicated than we thought previously.

In view of extremely low systemic bioavailability of CUR, the major site for metabolic interactions of CUR with other co-administered drugs is most likely in the intestine. As an inhibitor of MRP3 and P-gp, CUR can increase intracellular accumulation of cancer drug phosphor-sulindac in cancer cell lines A549 and SW480 through inhibition of the affected efflux transporters if concomitant use of the two drugs (Cheng, et al., 2013). Diclofenac acyl glucuronide is also a substrate of MRP3 (Scialis, et al., 2019). In addition, our recent work indicated that Mrp3 can transport clopidogrel acyl glucuronide from hepatocytes into the blood in mice (Ji, et al., 2018). When concurrent use of CUR and any other known MRP3 substrates or inhibitors, such as phosphor-sulindac, diclofenac (acyl glucuronide), or clopidogrel (acyl glucuronide), clinically important herb-drug interactions would occur. Of the all glucuronide conjugates, many are the MRP3 substrates, like COG identified in this work. Not limited to these cases, oral intake of CUR would significantly decrease the systemic bioavailability of CYP3A4 substrate drugs through activation of CYP3A4 by COG (Hsieh, et al., 2014). Therefore, metabolic interactions of CUR with other drugs seem to be more complex and clinically important than we thought.

In summary, this study reveals that COG is transported predominantly by the efflux transporter MRP3 in mice and is confirmed by the inverted recombinant membrane vesicle technique. These results suggest that herb-drug interactions might occur in patients concomitantly taking CUR and either an MRP3 substrate/inhibitor, or a drug that undergoes the glucuronidation pathway or whose

metabolism is catalyzed by CYP3A4 predominantly. These new findings would help enrich and update our knowledge of drug transporters and drug transport for better understanding of the interplay between drug transport and drug metabolism in the body. In view of the widespread use of GUR globally, such herb-drug interactions are of clinical importance.

Acknowledgments

The authors thank Dr. Piet Borst, Dr. Koen van de Wetering, Sin-Ming Sit (office manager for research), Frank Hoorn (office manager for technology transfer), and Carla Rijnders, the Netherlands Cancer Institute, Amsterdam, the Netherlands, for their generously providing MRP3 KO mice and expert assistance, and Mr. Michael B. Xie, Martin Luther King Jr. Magnet High School, Nashville, TN, USA, for his critical proof reading of the manuscript.

DMD Fast Forward. Published on January 3, 2020 as DOI: 10.1124/dmd.119.089193
This article has not been copyedited and formatted. The final version may differ from this version.

Disclosure of Conflicts of Interest

The authors have no conflicts of interest to declare.

Authorship Contributions

Participated in study design: Xie, Jia.

Conducted experiments: Jia, Zhu, Zhou, Ji, Tai.

Performed data analysis: Jia, Xie.

Wrote or contributed to the writing of the manuscript: Xie, Jia.

References

Abe Y, Fujiwara R, Oda S, Yokoi T and Nakajima M (2011) Interpretation of the effects of protein kinase C inhibitors on human UDP-glucuronosyltransferase 1A (UGT1A) proteins *in cellulo*. *Drug Metab Pharmacokinet* **26**:256–265.

Anand P, Kunnumakkara AB, Newman RA and Aggarwal BB (2007) Bioavailability of curcumin: problems and promises. *Mol Pharm* **4**:807–818.

Bangphumi K, Kittiviriyakul C, Towiwat P, Rojsitthisak P and Khemawoot P (2016) Pharmacokinetics of curcumin diethyl disuccinate, a prodrug of curcumin, in Wistar rats. *Eur J Drug Metab Pharmacokinet* **41**:777–785.

Berginc K, Trontelj J, Basnet NS and Kristl A (2012) Physiological barriers to the oral delivery of curcumin. *Pharmazie* **67**:518–524.

Basu NK, Kole L, Basu M, McDonagh AF and Owens IS (2007) Targeted inhibition of glucuronidation markedly improves drug efficacy in mice: a model. *Biochem Biophys Res Commun* **360**:7–13.

Cheng KW, Wong CC, Mattheolabakis G, Xie G, Huang L and Rigas B (2013) Curcumin enhances the lung cancer chemopreventive efficacy of phospho-sulindac by improving its pharmacokinetics. *Int J Oncol* **43**:895–902.

Farzaei MH, Zobeiri M, Parvizi F, El-Senduny FF, Marmouzi I, Coy-Barrera E, Naseri R, Nabavi SM, Rahimi R and Abdollahi M (2018) Curcumin in liver diseases: A systematic review of the

cellular mechanisms of oxidative stress and clinical perspective. *Nutrients* **10**:E855. doi: 10.3390/nu10070855

Garcea G, Berry DP, Jones DJ, Singh R, Dennison AR, Farmer PB, Sharma RA, Steward WP and Gescher AJ (2005) Consumption of the putative chemopreventive agent curcumin by cancer patients: Assessment of curcumin levels in the colorectum and their pharmacodynamic consequences. *Cancer Epidemiol Biomarkers Prev* **14**:120–125.

Hoehle SI, Pfeiffer E and Metzler M (2007) Glucuronidation of curcuminoids by human microsomal and recombinant UDP-glucuronosyltransferases. *Mol Nutr Food Res* **51**:932–938.

Hsieh YW, Huang CY, Yang SY, Peng YH, Yu CP, Chao PD and Hou YC (2014) Oral intake of curcumin markedly activated CYP 3A4: in vivo and ex-vivo studies. *Sci Rep* **4**:6587.

Huang Y, Cao S, Zhang Q, Zhang H, Fan Y, Qiu F and Kang N (2018) Biological and pharmacological effects of hexahydrocurcumin, a metabolite of curcumin. *Arch Biochem Biophys* **646**:31–37.

Ireson CR, Jones DJ, Orr S, Coughtrie MW, Boocock DJ, Williams ML, Farmer PB, Steward WP and Gescher AJ (2002) Metabolism of the cancer chemopreventive agent curcumin in human and rat intestine. *Cancer Epidemiol Biomarkers Prev* **11**:105–111.

Irving GR, Howells LM, Sale S, Kralj-Hans I, Atkin WS, Clark SK, Britton RG, Jones DJ, Scott EN, Berry DP, Hemingway D, Miller AS, Brown K, Gescher AJ and Steward WP (2013) Prolonged biologically active colonic tissue levels of curcumin achieved after oral administration – A clinical pilot study including assessment of patient acceptability. *Cancer Prev Res (Phila)* **6**:119–128.

Ji JZ, Tai T, Huang BB, Gu TT, Mi QY and Xie HG (2018) Mrp3 transports clopidogrel acyl glucuronide from the hepatocytes into blood. *Drug Metab Dispos* **46**:151–154.

Karibe T, Imaoka T, Abe K and Ando O (2018) Curcumin as an in vivo selective intestinal breast cancer resistance protein inhibitor in Cynomolgus monkeys. *Drug Metab Dispos* **46**:667–679.

Kunati SR, Yang S, William BM and Xu Y (2018) An LC-MS/MS method for simultaneous determination of curcumin, curcumin glucuronide and curcumin sulfate in a phase II clinical trial. *J Pharm Biomed Anal* **156**:189–198.

Lee JH, Oh JH and Lee YJ (2012). Biliary excretion of curcumin is mediated by multidrug resistance-associated protein 2. *Biol Pharm Bull* **35**:777–780.

Lu D, Liu H, Ye W, Wang Y and Wu B (2017) Structure- and isoform-specific glucuronidation of six curcumin analogs. *Xenobiotica* **47**:304–313.

Mahale J, Howells LM, Singh R, Britton RG, Cai H and Brown K (2018a) An HPLC-UV method for the simultaneous quantification of curcumin and its metabolites in plasma and lung tissue: Potential for preclinical applications. *Biomed Chromatogr* e4280.

Mahale J, Singh R, Howells LM, Britton RG, Khan SM and Brown K (2018b) Detection of plasma curcuminoids from dietary intake of turmeric-containing food in human volunteers. *Mol Nutr Food Res* **62**:e1800267.

Ozawa H, Imaizumi A, Sumi Y, Hashimoto T, Kanai M, Makino Y, Tsuda T, Takahashi N and Kakeya H (2017) Curcumin beta-D-glucuronide plays an important role to keep high levels of free-form curcumin in the blood. *Biol Pharm Bull* **40**:1515–1524.

Roberts MS, Magnusson BM, Burczynski FJ and Weiss M (2002) Enterohepatic circulation: Physiological, pharmacokinetic and clinical implications. *Clin Pharmacokinet* **41**:751–790.

Scialis RJ, Aleksunes LM, Csanaky IL, Klaassen CD and Manautou JE (2019) Identification and characterization of efflux transporters that modulate the subtoxic disposition of diclofenac and its metabolites. *Drug Metab Dispos* **47**:1080–1092.

Seitz S, Kretz-Rommel A, Oude Elferink RP and Boelsterli UA (1998) Selective protein adduct formation of diclofenac glucuronide is critically dependent on the rat canalicular conjugate export pump (Mrp2). *Chem Res Toxicol* **11**:513–519.

Sharma RA, Steward WP and Gescher AJ (2007) Pharmacokinetics and pharmacodynamics of curcumin. *Adv Exp Med Biol* **595**:453–470.

Szymusiak M, Hu X, Leon Plata PA, Ciupinski P, Wang ZJ and Liu Y (2016) Bioavailability of curcumin and curcumin glucuronide in the central nervous system of mice after oral delivery of nano-curcumin. *Int J Pharm* **511**:415–423.

Tai T, Mi QY, Ji JZ, Yin Q, Pan YQ, Zhang MR, Huang BB and Xie HG (2016) Enhanced platelet response to clopidogrel in Abcc3-deficient mice due to its increased bioactivation. *J Cardiovasc Pharmacol* **68**:433–440.

Volak LP and Court MH (2010) Role for protein kinase C delta in the functional activity of human UGT1A6: implications for drug-drug interactions between PKC inhibitors and UGT1A6. *Xenobiotica* **40**:306–318.

Zelcer N, van de Wetering K, de Waart R, Scheffer GL, Marschall HU, Wielinga PR, Kuil A, Kunne C, Smith A, van der, Valk M, Wijnholds J, Elferink RO and Borst P (2006) Mice lacking Mrp3 (Abcc3) have normal bile salt transport, but altered hepatic transport of endogenous glucuronides. *J Hepatol* **44**:768–775.

Footnotes:

a) Unnumbered footnote:

This work was supported in part by the National Natural Science Foundation of China [Grant 81473286 to H.-G.X.]; and Nanjing First Hospital [Grant 31010300010339 to H.-G.X.]. Dr. Xie is the recipient of the Distinguished Medical Experts of the Province of Jiangsu, China.

b) Unnumbered footnote:

Address correspondence to: Dr. Hong-Guang Xie, General Clinical Research Center, Nanjing First Hospital, Nanjing Medical University, 68 Changle Road, Nanjing 210006, People's Republic of China. E-mail: hongg.xie@gmail.com or hong-guang.xie@njmu.edu.cn

c) Numbered footnote:

Yu-Meng Jia [1], Ting Zhu [2], Huan Zhou [3], Jin-Zi Ji [4], Ting Tai [5], and Hong-Guang Xie [6]

Legends for Figures

Fig. 1. Chemical structures of curcumin (A) and curcumin-*O*-glucuronide (B).

Fig. 2. Mean plasma COG concentration−time curves in Mrp3 KO and WT mice after oral administration of 200 mg/kg of curcumin. Data are presented as mean ± SD, n = 8 each. COG, curcumin-*O*-glucuronide.

Fig. 3. The liver-to-plasma ratios of COG and CUR (**A**) and the COG-to-CUR ratio in plasma and liver (**B**) between Mrp3 KO and WT mice. Data are presented as mean ± SD, n = 8 each. $^{***}P$ < 0.001 vs. WT mice. Unpaired Student's t test. COG, curcumin-*O*-glucuronide; CUR, curcumin.

Fig. 4. The ATP-dependent uptake of COG into the inverted recombinant human MRP3 membrane vesicles. (**A**) Uptake activity of COG and $E_2$17βG in the presence of ATP or AMP. (**B**) Uptake ratio of COG and $E_2$17βG in the presence of ATP versus AMP. Transport was measured after 5 min of uptake at 37°C in the presence of 1 or 10 μM COG. $E_2$17βG (4 μM) was used as a positive substrate for MRP3. Data are presented as mean ± SD (n = 3 each). $^{*}P$ < 0.05, $^{**}P$ < 0.01, and $^{***}P$ < 0.001 vs. AMP group. Unpaired Student's t test. AMP, adenosine monophosphate; ATP, adenosine triphosphate; COG, curcumin-*O*-glucuronide; $E_2$17βG, estradiol-17β-D-glucuronide.

Fig. 5. Differences in the mRNA expression levels of *Abcc1*, *Abcc2*, *Abcc3*, and *Abcg2* in the liver (A) and intestine (B) of *Abcc3*/Mrp3 KO and WT mice. Data are presented as mean ± SD (n = 6 each). $^{***}P$ < 0.001 vs. Mrp3 WT group. Unpaired Student's t test.

DMD Fast Forward. Published on January 3, 2020 as DOI: 10.1124/dmd.119.089193
This article has not been copyedited and formatted. The final version may differ from this version.

Table 1. The pharmacokinetic parameters of COG in Mrp3 WT and KO mice after oral administration of 200 mg/kg of CUR.

Parameter	Unit	WT	KO
C_{max}	ng/mL	108.0 ± 28.6	3.3 ± 1.6 ***
T_{max}	min	195 ± 62.1	255 ± 100.1
AUC_{0-t}	ng·h /mL	655.7 ± 243.7	25.3 ± 11.0 ***
$AUC_{0-\infty}$	ng·h /mL	750.5 ± 235.9	27.3 ± 12.6 ***
$t_{1/2}$	min	162.1 ± 69.0	300.8 ± 124.6 *
MRT_{0-t}	min	293.6 ± 100.3	373.0 ± 72.2
$MRT_{0-\infty}$	min	328.0 ± 109.2	433.4 ± 119.1

Data are presented as mean ± SD (n = 8 each). $^{*}P < 0.05$, $^{***}P < 0.001$ vs. WT mice. Unpaired Student's t test. AUC_{0-t}, the area under the plasma drug concentration-time curve at last time point measured; $AUC_{0-\infty}$, the area under the plasma drug concentration-time curve extrapolated to infinity; C_{max}, maximum plasma drug concentration; MRT, mean residence time; $t_{1/2}$, (elimination phase) half-life; T_{max}, time to reach the peak plasma drug concentration.

DMD Fast Forward. Published on January 3, 2020 as DOI: 10.1124/dmd.119.089193
This article has not been copyedited and formatted. The final version may differ from this version.

A

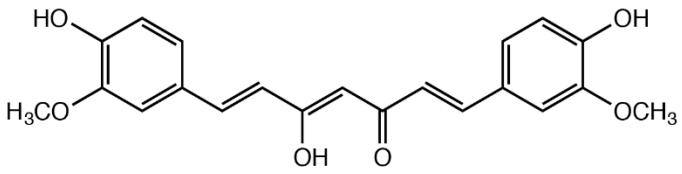

B

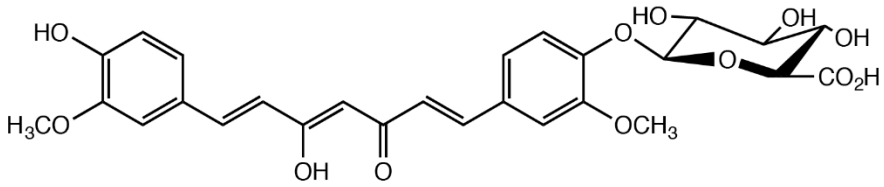

Fig. 1.

DMD Fast Forward. Published on January 3, 2020 as DOI: 10.1124/dmd.119.089193
This article has not been copyedited and formatted. The final version may differ from this version.

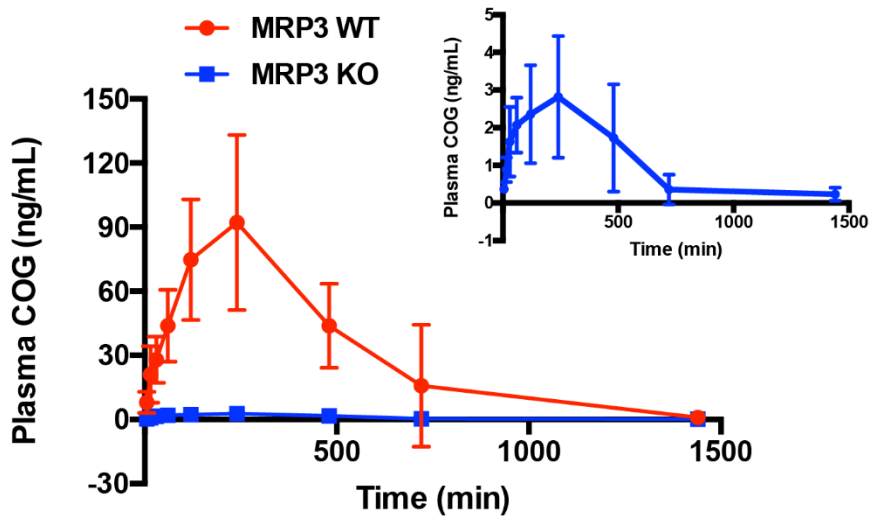

Fig. 2.

DMD Fast Forward. Published on January 3, 2020 as DOI: 10.1124/dmd.119.089193
This article has not been copyedited and formatted. The final version may differ from this version.

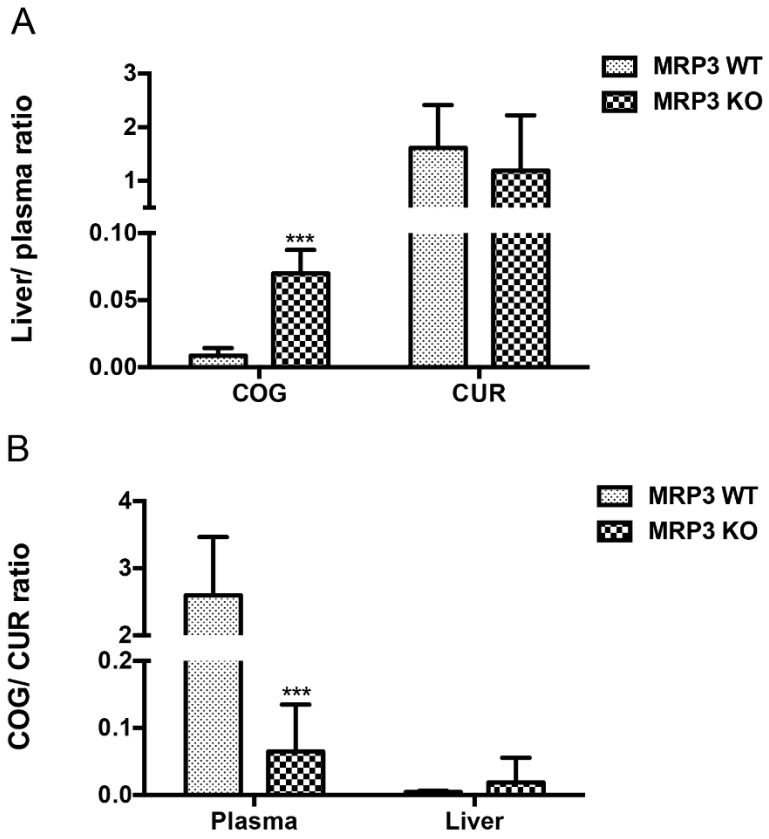

Fig. 3.

DMD Fast Forward. Published on January 3, 2020 as DOI: 10.1124/dmd.119.089193
This article has not been copyedited and formatted. The final version may differ from this version.

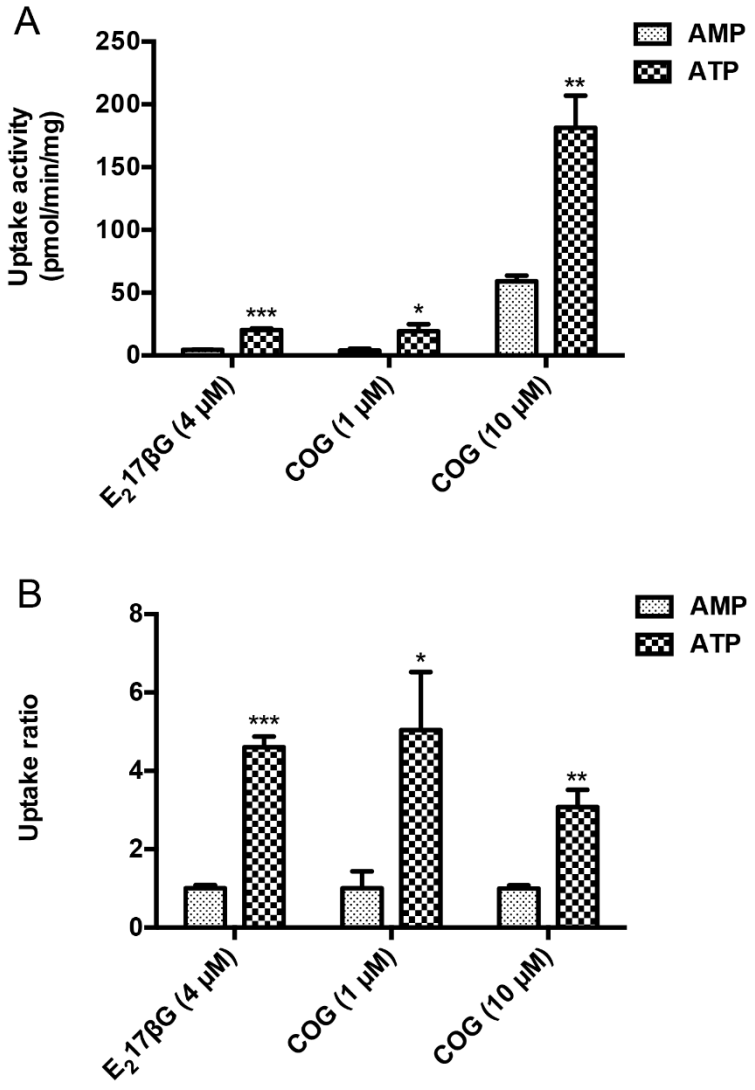

Fig. 4.

DMD Fast Forward. Published on January 3, 2020 as DOI: 10.1124/dmd.119.089193
This article has not been copyedited and formatted. The final version may differ from this version.

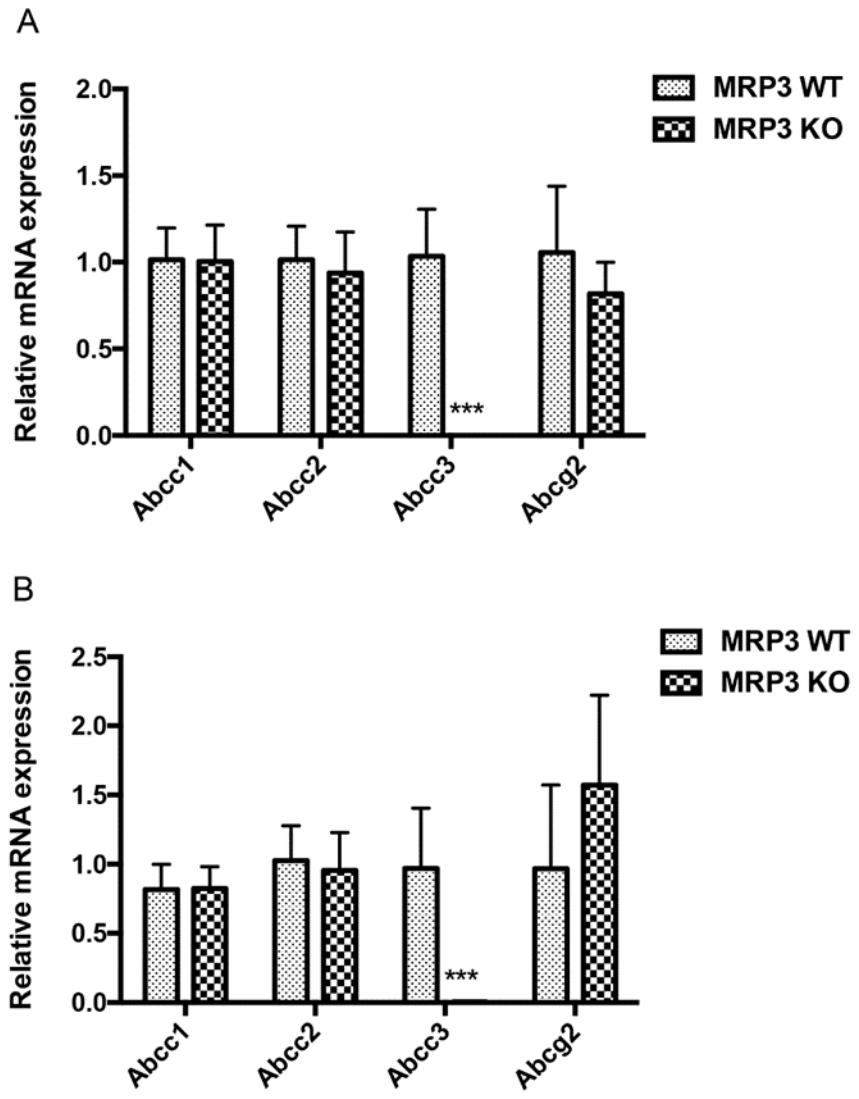

Fig. 5.